DNA stretch during electrophoresis due to a step change in mobility

Patrick T. Underhill* and Patrick S. Doyle†
Department of Chemical Engineering, Massachusetts Institute of Technology, Cambridge, Massachusetts 02139, USA
(Received 19 January 2007; published 19 July 2007)

We investigate DNA stretching during electrophoresis when the mobility abruptly changes. This is a simplified geometry that produces a nonhomogeneous strain rate over the scale of a single molecule. An effective Weissenberg number (Wi) and Deborah number were identified, and the degree of stretching was examined as a function of these two parameters. The system does not undergo a coil-stretch transition. The finite extensibility of the chains only affects the response if the chain is stretched to a significant fraction of the contour length. The wormlike chain shows a characteristic approach to full extension of $\mathrm{Wi}^{-1/2}$.

DOI: 10.1103/PhysRevE.76.011805 PACS number(s): 36.20.−r, 83.50.−v, 87.15.−v

I. INTRODUCTION

Mechanical models have been used widely to represent the behavior of polymers in flow. Many of the flows which have been considered previously are homogeneous in that the strain rate is the same everywhere in space, such as uniform shear or elongational flow. Even in a macroscopic complex geometry, at the scale of a single polymer molecule, the strain rate is homogeneous in space, although the flow can change in time in a Lagrangian sense. This is a result of the difference in scales between the size of the device and the size of a polymer molecule. However, a number of microfluidic devices involving biological polymers, such as double-stranded DNA, produce nonhomogeneous strain rates over the scale of a molecule. Examples of this type of flow include DNA separation devices using post arrays [1] or entropic traps [2] and DNA stretching devices for genome mapping [3]. A number of studies have been performed on polymers in nonhomogeneous flows. For example, Szeri *et al.* [4] examined deformable bodies in two-dimensional nonhomogeneous flows to understand the strong flow criterion. A number of different groups have performed Brownian dynamics simulations of polymers using an imposed, known flow field which is nonhomogeneous, and the dynamics and stretching of the polymer have been examined [5–7]. Randall *et al.* [8] have recently examined experimentally the stretching of DNA using nonhomogeneous fields generated using micro-contractions or the stretching as the DNA exits from a gel into aqueous solution.

The number of possible different nonhomogeneous problems is quite large. In general it is important to include the details of this nonhomogeneous field. Our approach is to examine a simplified system which contains the required physics of a nonhomogeneous strain rate over the scale of the molecule inspired by the experiments of Randall *et al.* [8]. The system is simple enough that some analytical progress can be made but also allows us to learn aspects such as the important dimensionless groups that apply to more complicated situations. The simplified geometry we consider is a step increase in the electrophoretic velocity, which is illustrated in Fig. 1. Under the conditions of electrohydrodynamic equivalence [9,10], the response to a hydrodynamic flow with velocity v is the same as to an electric field if the hydrodynamic velocity is replaced by the electrophoretic velocity μE, where μ is the mobility. Therefore, the electrophoretic velocity μE is the nonhomogeneous field we consider. Note that the step change in "field" could be accomplished either by a step change in electric field or mobility or a combination of both.

The problem which most resembles this geometry is the exit of a DNA molecule from a gel (region 1) to aqueous solution (region 2) [8], although our simplified geometry does not contain any structure in region 1 to describe details of the gel. The gel would simply act as a method of changing the electrophoretic velocity. The geometry could also represent the change of field that occurs in sharp constrictions such as entropic traps or hyperbolic contractions, although those geometries have additional steric hindrance not included here.

Our analysis will show that in a limiting case this geometry reduces to a tethered chain in a uniform flow, a problem which has received significant attention. Brochard-Wyart and co-workers [11,12] have used blob theory to examine the stretching and unwinding of tethered polymers. The validity of the blob theory has been investigated using Brownian dynamics simulations by Zimmermann and co-workers [13].

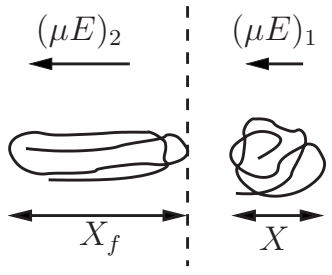

FIG. 1. The polymer is moving from right to left, initially with electrophoretic velocity $(\mu E)_1$. The maximum extent in the x direction is denoted by X. The chain crosses the dashed line into a region with electrophoretic velocity $(\mu E)_2 > (\mu E)_1$. The maximum extent of the polymer when the rear crosses the dashed line is defined as X_f.

*Present address: Department of Chemical and Biological Engineering, University of Wisconsin—Madison, Madison, WI 53706, USA.
†pdoyle@mit.edu

Brownian dynamics simulations have also been used to investigate the validity of a dumbbell model for a tethered chain [14] and to examine the dynamics of tethered chains in shear flow [15].

We will first examine a toy model consisting of a single Hookean dumbbell neglecting Brownian motion and hydrodynamic interactions to derive the dimensionless groups governing the response. A similar type of toy model can be used to understand the coil-stretch transition in elongational flow as reviewed in Ref. [16]. We will then show with Brownian dynamics simulations that the Hookean chains in the long chain limit converge to a result which has the same scaling as the toy model. Finally, we will show the effect that finitely extensible springs have on the result.

II. DUMBBELL MODEL

Here we will discuss a toy model which considers a single Hookean spring without Brownian motion or hydrodynamic interactions. The system is sketched in Fig. 1. The polymer is moving in region 1 with an electrophoretic velocity $(\mu E)_1$ and crosses into a region with electrophoretic velocity $(\mu E)_2$. For this discussion we consider $(\mu E)_2 > (\mu E)_1$, which causes the polymer to stretch in the x direction. The stretch when the last segment of polymer crosses from region 1 to 2 is defined as X_f. By using this toy model we can understand how this stretch scales with the properties of the chain and strength of the two velocities. In this way we can understand the physical mechanism involved in stretching.

To calculate the response of the dumbbell, we write down a force balance for each bead neglecting inertia, Brownian motion, hydrodynamic interaction, and electrostatic interaction between the beads. This is analogous to Long and Ajdari [17] who examined the mobility of composite objects. In Ref. [17], they neglected hydrodynamic and electrostatic interactions between segments with different mobilities. They were concerned with calculating the steady mobility of the composite object. The situation here is by necessity transient thus we are not concerned with calculating a mobility of the whole chain. Time zero is taken to be the first time one of the beads crosses from region 1 into region 2. This bead is denoted α while the other bead is denoted β. Using electrohydrodynamic equivalence and within the assumptions mentioned above the equations of motion are

$$\frac{dx_\alpha}{dt} = \frac{-1}{\zeta(x_\alpha)} H(x_\alpha - x_\beta) + (\mu E)(x_\alpha), \tag{1}$$

$$\frac{dx_\beta}{dt} = \frac{1}{\zeta(x_\beta)} H(x_\alpha - x_\beta) + (\mu E)(x_\beta), \tag{2}$$

where H is the linear spring constant and the drag coefficient on a bead ζ and the electrophoretic velocity μE can be a function of position. The situation in Fig. 1 considers a step change in μE and possibly a step change in ζ. The initial condition is that $x_\alpha(0)=0$ and $x_\beta(0)=-X_0$. Prior to $t=0$, the spring is at equilibrium, so X_0 is a random variable taken from a half-Gaussian. The integration forward in time is split into two types, depending on the value of X_0. If X_0 is small, dx_α/dt will be positive, and there will be a range of times $0<t<t_f$ for which $x_\alpha>0$ and $x_\beta<0$. With these restrictions we can calculate $X \equiv x_\alpha - x_\beta$ to be

$$X(t) = \frac{\delta_{\mu E}\zeta^*}{2H} - \left(\frac{\delta_{\mu E}\zeta^*}{2H} - X_0\right)\exp[-t2H/\zeta^*], \tag{3}$$

where we define an averaged drag coefficient as

$$\frac{1}{\zeta^*} = \frac{1}{2}\left(\frac{1}{\zeta_1} + \frac{1}{\zeta_2}\right), \tag{4}$$

ζ_1 and ζ_2 are the drag coefficients on a bead in regions 1 and 2, respectively, and $\delta_{\mu E}=(\mu E)_2-(\mu E)_1$.

The final stretch can be calculated as $X_f \equiv X(t=t_f)$, where t_f is defined by $x_\beta(t_f)=0$. This condition for t_f becomes an algebraic equation that must be solved numerically

$$0 = -2 + \left[\left(\frac{\zeta^*}{\zeta_1}\right)\left(\frac{\delta_{\mu E}\zeta^*}{2HX_0}\right) + \left(\frac{(\mu E)_1\zeta^*}{HX_0}\right)\right]\frac{t_f 2H}{\zeta^*} + \left(\frac{\zeta^*}{\zeta_1}\right)\left[\left(\frac{\delta_{\mu E}\zeta^*}{2HX_0}\right) - 1\right]\left[\exp\left(\frac{-t_f 2H}{\zeta^*}\right) - 1\right]. \tag{5}$$

Once this equation is solved for t_f, the result can be placed into

$$X_f = \frac{\delta_{\mu E}\zeta^*}{2H} - \left(\frac{\delta_{\mu E}\zeta^*}{2H} - X_0\right)\exp[-t_f 2H/\zeta^*]. \tag{6}$$

This summarizes the procedure to calculate X_f for a value of X_0 such that the front part of the dumbbell moves forward. First, the value of t_f is calculated numerically from the algebraic Eq. (5). This value is then used in Eq. (6) to calculate the final value of the stretch. However, for large values of X_0 these two equations are not appropriate because the front bead can retract back into the first region.

This situation is not a problem, however. If we return to the general formula with position dependent drag and electrophoretic velocity we see there will exist a region of time from $0<t<t^*$ for which both beads are in the first region and have the same drag and electrophoretic velocity. This time t^* can also be calculated by solving numerically an algebraic equation

$$1 - \exp\left[\frac{-t^* 2H}{\zeta_1}\right] = \left[\frac{(\mu E)_1\zeta_1}{HX_0}\right]\frac{t^* 2H}{\zeta_1}. \tag{7}$$

At time t^* the front bead will reach the step change (at $x=0$) again. However, the value of the stretch will now be smaller. This new stretch can be calculated from

$$X_{0,\text{new}} = X_0 \exp\left[\frac{-t^* 2H}{\zeta_1}\right]. \tag{8}$$

This value of the stretch is small enough that the integration will now proceed exactly as in Eqs. (5) and (6) but now with a new value of the initial stretch $X_{0,\text{new}}$.

To this point we have discussed how the final value of the stretch X_f can be calculated for an initial value of the stretch X_0. The property of interest is the average value of X_f given a distribution of initial stretch X_0. This is calculated simply as

$$\langle X_f \rangle = \int_0^\infty X_f P(X_0) dX_0, \tag{9}$$

where $P(X_0)$ is the probability distribution of initial stretch and is given by a half-Gaussian because of the linear spring force law.

Throughout Eqs. (5), (6), (7), and (8) we have seen that two parameters greatly affect the response. These two parameters are

$$\frac{\delta_{\mu E}\zeta^*}{2HX_{0,\mathrm{typ}}}, \tag{10}$$

$$\frac{(\mu E)_1\zeta^*}{HX_{0,\mathrm{typ}}}, \tag{11}$$

where $X_{0,\mathrm{typ}}$ is a typical value of the initial stretch. For the linear springs this typical value is taken to be

$$X_{0,\mathrm{typ}} = \sqrt{k_B T/H}. \tag{12}$$

In order to compare this toy model with the response of bead-spring chains and models including finite extensibility, we need to generalize these parameters to other types of chains. We choose to do this by replacing

$$\zeta^*/H \to 4\tau, \tag{13}$$

$$X_{0,\mathrm{typ}} \to \sqrt{\langle R^2 \rangle_{\mathrm{eq}}/3}, \tag{14}$$

where τ is the longest relaxation time if each bead had drag coefficient ζ^* and $\langle R^2 \rangle_{\mathrm{eq}}$ is the equilibrium averaged end-to-end distance squared of the chain. With these substitutions the two parameters become

$$\mathrm{Wi} = \frac{\delta_{\mu E} 2\tau}{\sqrt{\langle R^2 \rangle_{\mathrm{eq}}/3}}, \tag{15}$$

$$\mathrm{De} = \frac{(\mu E)_1 4\tau}{\sqrt{\langle R^2 \rangle_{\mathrm{eq}}/3}}. \tag{16}$$

The first of these parameters is a Wiessenberg number because the chain sees a difference in the electrophoretic velocity of $\delta_{\mu E}=(\mu E)_2-(\mu E)_1$ over the size of the polymer. The ratio of these gives an effective strain rate which is used to calculate a Weissenberg number. This is not like a typical elongational flow, though, for two reasons. First, as the chain extends, the same difference in velocities is seen by the chain over a larger distance, resulting in a decreasing effective strain rate as the chain stretches. This continues until the stretching provided by the change in velocity exactly cancels the spring force trying to resist stretching. Second, the chain only has a finite residence time across the step change. Once the rear of the chain passes over the step change in electrophoretic velocity, the chain relaxes back to the equilibrium state. The finite residence time is due both to the fact that the front of the molecule is pulling the back across the interface and to the fact that the back is being convected across the interface. Thus the velocity in region 1 also plays a role, which comes in through the Deborah number (De). This is a Deborah number because the residence time to cross the interface is typically of order $\sqrt{\langle R^2 \rangle_{\mathrm{eq}}/3}/(\mu E)_1$ because Brownian motion has been neglected in the toy model. This convective time scale introduces another flow time scale which can be compared to the relaxation time, separate from the inverse strain rate, so we can define a Deborah number in addition to the Weissenberg number, which is always taken to be the product of the strain rate and the relaxation time [16,18].

Instead of also using a Deborah number, an effective strain can be defined as the ratio of the Weissenberg number to the Deborah number

$$\epsilon = \frac{\mathrm{Wi}}{\mathrm{De}} = \frac{\delta_{\mu E}}{2(\mu E)_1}. \tag{17}$$

This represents an effective strain because it is the product of the effective strain rate used in Wi and the residence time used in De. We will find that some situations are more naturally described using De while others with ϵ.

While these parameters play a key role, looking at Eq. (5) we see that how the drag coefficient changes across the interface also affects the response through the parameter ζ^*/ζ_1. We model the drag coefficient using the Stokes law formula $\zeta=6\pi\eta R$, where η is the effective viscosity of the medium and R is the radius of the bead. If the first region is a gel, this formula is a simplifying assumption in which we treat the gel as a Newtonian fluid with an effective viscosity. Because we are not allowing the radius of a bead to change as it crosses the step change, the drag coefficient only changes if the effective viscosity changes.

We must similarly consider how a change in effective viscosity would affect the mobility of a bead. Calculating the mobility of a bead *a priori* is a difficult task which is not the goal of this work nor is it necessary here. We are only concerned with how a change in the effective viscosity changes the mobility. Consider the Smoluchowski formula for the mobility of a sphere $\mu=\sigma/(\eta\kappa)$, where σ is the surface charge density, η is the effective viscosity of the medium, and κ^{-1} is the Debye length. The mobility is inversely proportional to the effective viscosity, which is expected if the deformation of the counterionic cloud can be neglected. Therefore in terms of the effective viscosity, the product $\zeta\mu$ is constant for a bead as it crosses the step change. Certainly this product will depend on the size of the bead, the Debye length, and many other parameters. However, we are assuming that the only thing allowed to change to affect the drag coefficient or mobility is the effective viscosity. With respect to this property, the product $\zeta\mu$ is constant. This allows us to relate the ratio ζ^*/ζ_1 to the parameters already defined.

As we mentioned previously, a step change in the "field" μE can result from a step change in E or μ or both. Although the way in which μE changes does not affect the value of μE in each region, it is only the change in μ (through a change in effective viscosity) that also affects the drag coefficient.

In the rest of this article we will consider the case in which $E_1=E_2$. The difference in electrophoretic velocity comes about because of a change in effective viscosity which affects the mobility. Because the electric field is the same

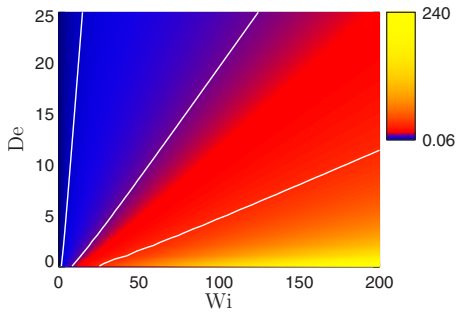

FIG. 2. (Color online) Contours of constant $\langle X_f\rangle/\langle X\rangle_{\mathrm{eq}}$ for the toy model as a function of the two parameters De and Wi. From left to right, the lines represent constant $\langle X_f\rangle/\langle X\rangle_{\mathrm{eq}}$ of 2, 10, and 30.

across the interface, the effective strain becomes $\epsilon=(\mu_2-\mu_1)/(2\mu_1)$. However, the change in effective viscosity means that $\zeta_1/\zeta_2=\mu_2/\mu_1$ as discussed in the past few paragraphs. Together, these relations become $\zeta^*/\zeta_1=1/(1+\epsilon)$. This is used in Eq. (5) when the response of the toy model is calculated.

This may seem like a strange system to consider as an example of a nonhomogeneous field because the electric field is actually constant everywhere. However, the concept of electrohydrodynamic equivalence tells us that it is not the electric field that plays the role of the externally imposed "flow field" but instead the product μE. This type of stretching in a uniform electric field by a change in mobility has been observed experimentally by Randall *et al.* [8]. They performed experiments observing DNA stretching as it exits from a gel into a region without a gel (from smaller mobility to larger mobility).

We can characterize the response of this model by examining the amount of stretching relative to equilibrium $\langle X_f\rangle/\langle X\rangle_{\mathrm{eq}}$ as a function of Wi and De, as shown in Fig. 2. In Fig. 3, we show the same data but in terms of Wi and ϵ.

The first key observation is the absence of a coil-stretch transition. Up to near a value of Wi=1 the toy model predicts no stretching beyond equilibrium because at this point the stretching is balanced by the spring force. Therefore, we see that below a value of about Wi=1 there is only minimal stretching. At larger Wi the stretch increases approximately linearly. The slope of this increase is determined by De.

The affine limit is reached as the De becomes very large. In this region, the back part of the chain is simply convected

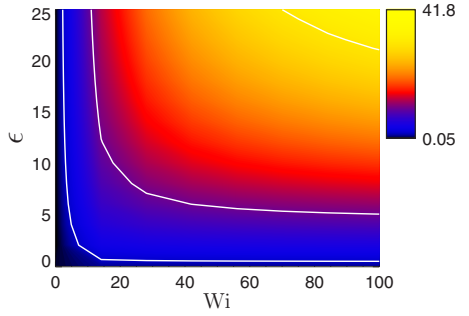

FIG. 3. (Color online) Contours of constant $\langle X_f\rangle/\langle X\rangle_{\mathrm{eq}}$ for the toy model as a function of the two parameters ϵ and Wi. From left to right, the lines represent constant $\langle X_f\rangle/\langle X\rangle_{\mathrm{eq}}$ of 2, 10, and 30.

to the interface. The final stretch is the distance the front of the chain travels in the time it takes for the back part to reach the interface. In this limit the toy model gives

$$\frac{\langle X_f\rangle}{\langle X\rangle_{\mathrm{eq}}} \sim 1+\frac{2\mathrm{Wi}}{\mathrm{De}}=1+2\epsilon. \tag{18}$$

The key observation in this region is that the stretch is only a function of the ratio Wi/De, or the strain ϵ. Therefore, the details of the polymer in terms of the coil size and relaxation time and the applied electric field are irrelevant in determining the relative stretch from the equilibrium state. In this region the stretch is simply a function of the ratio μ_2/μ_1. This region can be seen in Fig. 3. The lower-right region ($\mathrm{Wi}\gg\epsilon$) corresponds to the affine limit ($\mathrm{De}\gg 1$). The contours become flat, which means the stretch is independent of Wi, and only depends on ϵ.

In the limit of very small De, the response approaches that of a tethered chain. In this region the toy model gives

$$\frac{\langle X_f\rangle}{\langle X\rangle_{\mathrm{eq}}} \propto \mathrm{Wi}. \tag{19}$$

The mobility in region 1 is small enough that the chain in region 2 reaches a "steady" or balanced configuration in which the stretching due to the velocity difference is balanced by the spring force before the rear of the polymer crosses the interface. Note that in this limit the Wi could also be thought of as the Peclet number in the two regions because $\mathrm{De}\to 0$. For example, in this limit the average drag $\zeta^*\to 2\zeta_2$, and the relaxation time could be related to a diffusivity using scaling relations [19]. Again this limit can be easily seen in Fig. 3. The upper-left region ($\epsilon\gg\mathrm{Wi}$) corresponds to small De. In this limit the contours become vertical, i.e., independent of ϵ and only dependent on Wi.

III. LONG CHAIN LIMIT

To verify that these scaling ideas hold even for polymer chains, with the additional complexity of back-folds and kinks, we performed Brownian dynamics simulations of bead-spring chains with Hookean springs. The details of the Brownian dynamics method are reviewed elsewhere [20]. We used a standard explicit Euler time-stepping scheme, but the change in drag coefficient, and therefore diffusivity, across the step change must be correctly included. We used the midpoint algorithm of Grassia *et al.* [21] which is able to account for this change.

Chains were simulated for increasing number of beads, and it was found that for $N\geq 40$ the results collapsed onto a single curve, and thus are in the long chain limit. These chains in the long chain limit were observed to have the same scaling with De and Wi as the toy model. This illustrates the validity of the two dimensionless groups and the regions in phase space discussed previously. It is not surprising that there is not quantitative agreement between the toy model and the chains which can form kinks and hairpins. Over a range of parameters it was found that a simple formula can relate the response of the long chains and the toy model. This approximation is defined by the equation

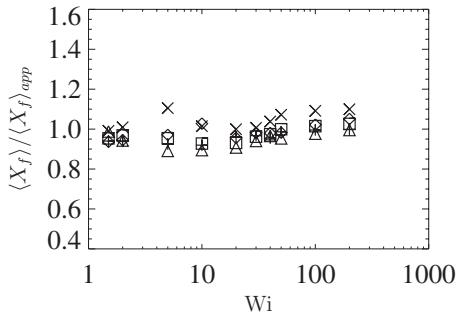

FIG. 4. This shows a comparison of Brownian dynamics simulations in the long chain limit to the toy model. We show the result of the simulations divided by the approximation in Eq. (20). The symbols represent values of De: 0.5 (crosses), 1.0 (squares), 2.0 (triangles), 5.0 (pluses), and 10.0 (diamonds).

$$\frac{\langle X_f \rangle_{\text{app}}}{\langle X \rangle_{\text{eq}}} \sim 1 + 0.6\left(\frac{\langle X_f \rangle_{\text{toy}}}{\langle X \rangle_{\text{eq}}} - 1 \right). \tag{20}$$

In Fig. 4 we show the ratio of the simulated stretch of the bead-spring chains with $N=40$ to this approximate formula versus Wi. We see that other than at very small De, this simple approximation works quite well. The prefactor of 0.6 and the slight change at small De are probably due to the tendency of chains to form hairpins which tend to reduce the extension relative to that seen with a dumbbell model.

IV. FINITE EXTENSIBILITY

To this point we have only considered Hookean springs, which can be infinitely extended. Real polymers, however, have a finite length. As the chain is extended to a significant fraction of that fully extended length, the spring force increases nonlinearly, ultimately diverging to prevent the chain from extending past the contour length. Typically this nonlinear increase in force begins when the extension is approximately one-third of the contour length. We expect that if the stretch experienced crossing the step change $\langle X_f \rangle$ is less than about one-third of the contour length, the finite extensibility does not influence the result. The stretch will be the same as with Hookean chains.

We performed a series of simulations of bead-spring chains with nonlinear springs, with some characteristic data shown in Fig. 5. The spring force law was developed previously [22] to model a worm-like chain polymer. The spring force law is

$$\hat{f}_s = \frac{\hat{r}}{(1-\hat{r}^2)^2} - \frac{7\hat{r}}{\nu(1-\hat{r}^2)} + \left(\frac{3}{32} - \frac{3}{4\nu} - \frac{6}{\nu^2} \right)\hat{r} + \left(\frac{\frac{13}{32} + \frac{0.8172}{\nu} - \frac{14.79}{\nu^2}}{1 - \frac{4.225}{\nu} + \frac{4.87}{\nu^2}} \right)\hat{r}(1-\hat{r}^2), \tag{21}$$

where the spring force is made dimensionless using the persistence length $\hat{f}_s = f_s A_p / (k_B T)$, the spring extension is written as the fractional extension of the spring $\hat{r}$, and ν is the number of persistence lengths represented by each spring.

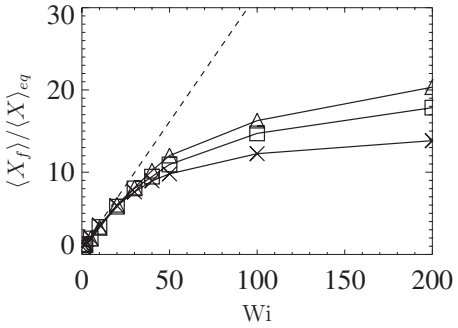

FIG. 5. Results from simulations with increasing finite extensibility. The Deborah number is De=2.0. The dashed line represents the approximation for Hookean chains in the long chain limit [Eq. (20)]. The symbols represent simulations for λ (crosses), 2λ (squares), and 3λ (triangles).

A common molecule used in single molecule video fluorescence microscopy experiments is λ-phage DNA which contains about 400 persistence lengths when stained with a fluorescent dye [23]. It is also common to examine concatemers which are twice and three times as long, which we call 2λ and 3λ. The result of simulations of these three molecules are shown in Fig. 5. The chains contain 20, 39, and 58 beads, respectively, so that the number of persistence lengths per spring is the same. The dashed line is the approximation to a long chain of Hookean springs [Eq. (20)]. For the nonlinear bead-spring chains with a large number of beads, we expect that at small extensions the simulations follow the Hookean chain result. As the extension grows, it eventually reaches a significant fraction of the contour length. At this point the nonlinearity in the spring makes the extension less than that predicted from the Hookean model which was valid at small extensions. The finite extensibility for longer contour length chains does not influence the result until larger Wi as seen in Fig. 5.

At large enough Wi the extension will approach the contour length of the polymer L. A characteristic of the worm-like chain in elongational flow is that the approach to full extension follows the power law $\text{Wi}^{-1/2}$. This is distinguished from the approach for the freely jointed chain which follows Wi^{-1}. This same power law has also been observed for the stretching of tethered DNA in uniform flow, which can be generated either by hydrodynamic or electrophoretic forces [24–26]. For a tethered wormlike chain in shear flow, it has been shown that the approach to full extension follows the power law $\text{Wi}^{-1/3}$ [15]. In Fig. 6 we show the approach to full extension for the case of λ DNA modeled with 20 beads. We see that for both De=2 and De=5 if the stretch is greater than about $0.3L$, the finite extensibility is important and the approach to full extension decays as $\text{Wi}^{-1/2}$.

This influence of finite extensibility can also be understood in terms of the phase plot given in Figs. 2 and 3. For a given molecule of interest, a curve of constant stretch can be placed on the phase plot which corresponds to a significant fraction of the contour length, such as one-third. From force-extension results for flexible polymers we know the nonlin-

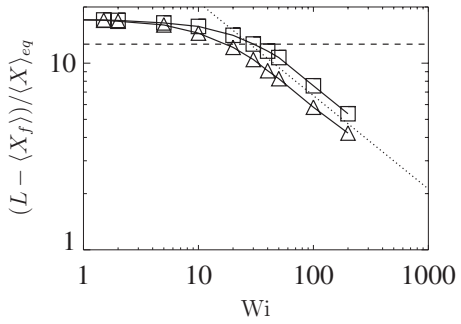

FIG. 6. Approach of the nonlinear bead-spring chains to full extension. The chain contains 20 beads and 400 persistence lengths in the whole chain. The data corresponds to De of 2 (triangles) and 5 (squares). The dotted line is a power law of $\mathrm{Wi}^{-1/2}$. The dashed line represents a value of $\langle X_f\rangle = 0.3L$.

earity begins influencing the stretch at about this point. In the region with stretch less than this value, a simple Hookean chain can correctly model the stretch experienced. On the other side of the curve, the nonlinearity will limit the stretch to a smaller value than that predicted by a Hookean theory. For molecules of increasing contour length, this curve will be pushed to higher Wi and smaller De. Thus for increasingly long polymers, more of the region of phase space will be correctly modeled using a Hookean chain.

V. CONCLUSIONS

In this paper, we have discussed a simplified system which has a nonhomogeneous strain rate over the scale of a single polymer molecule. We used a toy model of a single Hookean spring without Brownian motion to identify a Weissenberg number and Deborah number. We showed that the stretch of Hookean chains in the long chain limit still scale with these two parameters. The change in velocity divided by the size of the molecule as the effective strain rate. The chain stretching is also a transient process, with a finite residence time experiencing the stretching force.

These two dimensionless groups formed a phase space which we examined. For $\mathrm{Wi} \lesssim 1$ the chain experiences minimal stretching. Above $\mathrm{Wi}=1$ there is an approximate linear increase of stretch with Wi. For large De, this increase follows the affine limit scaling. For very small De, the system approaches a tethered limit, in which the chain has time to reach a "steady" balance between the velocity difference which is trying to stretch the chain and the spring force which is trying to relax the chain. If chains are stretched to greater than approximately one-third of the contour length, the finite extensibility of the chain is important. We showed a characteristic approach of $\mathrm{Wi}^{-1/2}$ to full extension for the wormlike chain.

These same dimensionless groups and this type of phase space analysis should also provide insight into other more complex flow geometries in which the flow has nonhomogeneous strain rates over the scale of a single molecule as well as transient flows. These types of flows should become even more prevalent in single molecule studies in microfluidic devices. Recent experimental studies observing the stretching of DNA as it moves through a contraction have been performed using hydrodynamic flows [27] and electric fields [3,8]. Computer simulations have also been done recently for the case of electric fields [28] to understand which designs produce the maximum stretching of the DNA. These simulations analyzed the stretching of DNA undergoing electrophoresis in different channel contractions. The gradients in the electric field cause stretching of the DNA. One observation from those simulations can be understood using the analysis we have presented. In the nomenclature of this article, the contraction may act similarly to an increase in electric field $E_2 > E_1$ with no change of the mobility or drag coefficient. As the electric field is increased, both Wi and De increase because the device essentially operates at constant effective strain ϵ. In this limit they see a maximum obtained stretching which is less than the contour length. This can be understood by looking at a plot similar to the one in Fig. 3. Because the experiments are performed at constant strain, the infinite Wi limit is given by the affine result.

ACKNOWLEDGMENTS

This work was supported by the National Science Foundation CAREER program Grant No. CTS-0239012 and P.S.D. acknowledges support from the Doherty Chair.

[1] W. D. Volkmuth and R. H. Austin, Nature (London) **358**, 600 (1992).
[2] J. Han and H. Craighead, Science **288**, 1026 (2000).
[3] K. M. Phillips, J. W. Larson, G. R. Yantz, C. M. D'Antoni, M. V. Gallo, K. A. Gillis, N. M. Goncalves, L. A. Neely, S. R. Gullans, and R. Gilmanshin, Nucleic Acids Res. **33**, 5829 (2005).
[4] A. Szeri, S. Wiggins, and L. Leal, J. Fluid Mech. **228**, 207 (1991).
[5] A. Panwar and S. Kumar, J. Chem. Phys. **118**, 925 (2003).
[6] M. Chopra, L. Lei, H. Hu, M. Burns, and R. Larson, J. Rheol. **47**, 1111 (2003).
[7] R. Duggal and M. Pasquali, J. Rheol. **48**, 745 (2004).
[8] G. Randall, K. Schultz, and P. Doyle, Lab Chip **6**, 516 (2006).
[9] D. Long, J.-L. Viovy, and A. Ajdari, Phys. Rev. Lett. **76**, 3858 (1996).
[10] G. Randall and P. Doyle, Macromolecules **38**, 2410 (2005).
[11] F. Brochard-Wyart, Europhys. Lett. **23**, 105 (1993).
[12] F. Brochard-Wyart, H. Hervet, and P. Pincus, Europhys. Lett. **26**, 511 (1994).
[13] R. Rzehak, W. Kromen, T. Kawakatsu, and W. Zimmermann, Eur. Phys. J. E **2**, 3 (2000).
[14] R. G. Larson, T. T. Perkins, D. E. Smith, and S. Chu, Phys. Rev. E **55**, 1794 (1997).

[15] B. Ladoux and P. Doyle, Europhys. Lett. **52**, 511 (2000).
[16] T. Squires and S. Quake, Rev. Mod. Phys. **77**, 977 (2005).
[17] D. Long and A. Ajdari, Electrophoresis **17**, 1161 (1996).
[18] R. Larson, J. Rheol. **49**, 1 (2005).
[19] P. deGennes, *Scaling Concepts in Polymer Physics* (Cornell University Press, Ithaca, NY, 1979).
[20] H. Öttinger, *Stochastic Processes in Polymeric Fluids: Tools and Examples for Developing Simulation Algorithms* (Springer, Berlin, 1996).
[21] P. Grassia, E. Hinch, and L. Nitsche, J. Fluid Mech. **282**, 373 (1995).
[22] P. Underhill and P. Doyle, J. Rheol. **50**, 513 (2006).
[23] P. Underhill and P. Doyle, J. Non-Newtonian Fluid Mech. **122**, 3 (2004).
[24] J. Marko and E. Siggia, Macromolecules **28**, 8759 (1995).
[25] T. Perkins, D. Smith, R. Larson, and S. Chu, Science **268**, 83 (1995).
[26] S. Ferree and H. Blanch, Biophys. J. **85**, 2539 (2003).
[27] P. J. Shrewsbury, S. J. Muller, and D. Liepmann, Biomed. Microdevices **3**, 225 (2001).
[28] J. Kim and P. Doyle, Lab Chip **7**, 213 (2007).